# A proton–hydride diiron complex with a base-containing diphosphine ligand relevant to the [FeFe]-hydrogenase active site†

**Ning Wang,[a] Mei Wang,*[a] Tingting Zhang,[a] Ping Li,[a] Jihong Liu[a] and Licheng Sun*[ab]**

*Received (in Cambridge, UK) 3rd July 2008, Accepted 20th August 2008*
*First published as an Advance Article on the web 1st October 2008*
**DOI: 10.1039/b811352a**

**A diiron dithiolate complex holding a μ-hydride on the iron atoms and a proton on the basic site of a chelating diphosphine ligand was prepared and crystallographically characterized as a structural model of the [FeFe]-hydrogenase active site, and its molecular structure shows the $H_{\mu}^{-}\cdots H_{N}^{+}$ distance is 3.934 Å.**

The chemistry of diiron dithiolate complexes is of interest to many chemists for understanding [FeFe]-hydrogenases ([FeFe]-$H_2$ases) and for developing cheap and efficient iron-based dihydrogen production catalysts. Among the numerous synthetic model complexes, the diiron dithiolate complexes containing an internal base have drawn considerable attention as an internal base may act as a proton relay to form a proton–hydride intermediate.[1–8] This intermediate is an inevitable state in the processes of the proton reduction and the dihydrogen oxidation *via* an ionic mechanism.

Spectroscopic evidence has proved that the protonation of the bridging N atom of all-carbonyl diiron azadithiolate complexes occurred rapidly,[1,2] and two *N*-protonated diiron complexes were crystallographically characterized.[3,4] The μ-hydride diiron complexes have been prepared from the protonation of the diiron complexes containing strong electron donating ligands, such as $PR_3$,[9,10] $CN^-$,[11] and N-heterocyclic carbene (NHC).[12] Although the [$Fe^{II}$(μ-H)$Fe^{II}$] species exhibit no inherent reactivity toward proton reduction, DFT studies on heterolytic H–H formation/breaking at the diiron sub-cluster suggest that [$Fe^{II}$(μ-H)$Fe^{II}$] species may act as an intermediate state in the catalytic cycle of the H-cluster.[13,14] A terminal hydride [FeFeH] is proposed to be a major key intermediate in the $H_2$ activation process at the H-cluster. The first terminal hydride model complex was prepared indirectly by reduction of a diiron(II) complex.[15] Some terminal hydride species, formed by protonation of diiron complexes with LˆL chelating ligands (LˆL = $Ph_2PCH_2CH_2PPh_2$, *cis*-$Ph_2PCH{=}CHPPh_2$, bis(N-heterocyclic carbene)), were identified by *in situ* NMR spectra at low temperature (−90 to −20 °C).[12,16,17] They quickly transform to the thermodynamically stable μ-hydride isomers upon warming the solution.

In addition to single protonation, recently, the double protonation of diiron azadithiolate complexes, both at the iron centre and at the bridging N atom, have been spectroscopically characterized.[6,7,17] There is only one report on the double protonation at the iron centre and the σ-donor ligand ($CN^-$), resulting in a rather unstable species.[11] To the best of our knowledge, none of the proton–hydride models of the H-cluster have been isolated and crystallographically characterized so far. Here we report the successful isolation and the crystal structure of a proton–hydride diiron complex [(μ-H)(μ-pdt){$Fe(CO)_3$}{Fe(CO)-($\kappa^2$*P*,*P*′-PNPH)}]($OTf)_2$ ([**1**($H_NH_{\mu}$)]($OTf)_2$; pdt = propane-1,3-dithiolate, PNP = $Ph_2PCH_2N(n\text{-}Pr)CH_2PPh_2$), as well as the protonation process of [(μ-pdt){$Fe(CO)_3$}{Fe(CO)($\kappa^2$*P*,*P*′-PNP)}] (**1**) in the presence of HOTf. The N-bridged diphosphine ligand was chosen as it features chelating ability with a hydrophilic and basic site deemed to be valuable for functional modes of $H_2 \rightleftharpoons 2H^+ + 2e$.[18–20]

Treatment of [(μ-pdt)$Fe_2(CO)_6$] with PNP ligand in refluxing toluene afforded **1** as a brown solid in moderate yield (see ESI†). Complex **1** was doubly protonated in diethyl ether upon addition of 3 equiv. of HOTf. The proton–hydride diiron complex [**1**($H_NH_{\mu}$)]($OTf)_2$ was obtained as a purple crystalline solid in good yield after washing with diethyl ether and recrystallized in hexane–$CH_2Cl_2$. Complex **1** is stable in the solid state and in solution under an $N_2$ atmosphere, while its doubly protonated species [**1**($H_NH_{\mu}$)]($OTf)_2$ is very sensitive to moisture. Complexes **1** and [**1**($H_NH_{\mu}$)]($OTf)_2$ were characterized by IR, $^1H$ and $^{31}P$ NMR spectroscopy, as well as by elemental analysis and single crystal X-ray analysis.

The molecular structures of **1** and [**1**($H_NH_{\mu}$)]($OTf)_2$ are given in Fig. 1 (Fig. S1†).‡ The asymmetric unit in the crystal structure of [**1**($H_NH_{\mu}$)]($OTf)_2$ is comprised of a molecule of [**1**($H_NH_{\mu}$)]($OTf)_2$ and a molecule of $H_2O$ (Fig. S2 and Table S1 in ESI†). The butterfly framework of **1** and [**1**($H_NH_{\mu}$)]$^{2+}$ is closely analogous to other previously reported $Fe_2S_2$ complexes.[10–12] After protonation on the iron atoms, the Fe–Fe distance is increased by 0.056 Å and the coordination geometry around each iron atom changes from distorted square-pyramidal in **1** to octahedral in [**1**($H_NH_{\mu}$)]$^{2+}$. The PNP ligand chelates to the Fe(2) atom of **1** in a binding mode of the apical/basal position, while the two phosphorus atoms in [**1**($H_NH_{\mu}$)]$^{2+}$ are in an equatorial-chelating configuration. The different coordination modes lead to the single bond

[a] *State Key Laboratory of Fine Chemicals, DUT-KTH Joint Education and Research Centre on Molecular Devices, Dalian University of Technology (DUT), Dalian, 116012, China. E-mail: symbueno@dlut.edu.cn; Fax: +86 411 83702185; Tel: +86 411 88993886*
[b] *Department of Chemistry, Royal Institute of Technology (KTH), Stockholm, 10044, Sweden*

† Electronic supplementary information (ESI) available: Experimental details, molecular structures and packing diagram of [**1**($H_NH_{\mu}$)]($OTf)_2$, IR spectra and cyclic voltammograms (Fig. S1–S4). CCDC reference numbers 693384 and 693385. For ESI and crystallographic data in CIF or other electronic format see DOI: 10.1039/b811352a

 

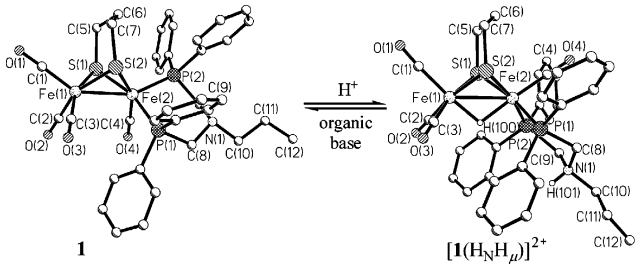


**Fig. 1** Molecular structures of **1** (left) and $[\mathbf{1}(H_NH_\mu)]^{2+}$ (right) as ball and stick drawings. Selected distances (Å) and angles (°) for **1**: Fe–Fe, 2.5565(7); Fe–S, 2.2527(10)–2.2644(11); Fe–P, 2.1981(10)–2.2132(11); Fe(1)–C, 1.786(5)–1.790(4); Fe(2)–C, 1.747(4); N–C, 1.456(5)–1.465(5); P(1)–Fe–P(2), 92.51(4); for $[\mathbf{1}(H_NH_\mu)]^{2+}$: Fe–Fe, 2.6120(16); Fe–S, 2.2493(16)–2.2593(16); Fe–P, 2.2185(17)–2.2319(15); Fe–H, 1.65(4)–1.70(3); Fe(1)–C, 1.799(6)–1.816(6); Fe(2)–C, 1.740(5); N–H, 0.90(3); N–C, 1.485(5)–1.509(5); P(1)–Fe–P(2), 95.82(6); Fe(1)–H–Fe(2), 102.8.

rotation of the Fe(2)PCNCP cyclohexane ring. The Fe(2) atom points down and the N atom is up in the chair conformation of **1**, while a rotated chair conformation is observed for $[\mathbf{1}(H_NH_\mu)]^{2+}$ with the hydrogen attached to the nitrogen atom on the axial bond. The $H_N{\cdot}H_\mu$ distance is 3.934 Å in the molecule of the doubly protonated species.

Complex **1** in $CH_2Cl_2$ solution displays three $\nu$(CO) bands at 2020, 1948, and 1894 $cm^{-1}$ in the IR spectrum (Fig. S3(a)†). Upon addition of 0.7 equiv. of HOTf to the solution of **1**, two new $\nu$(CO) bands, shifted to higher energy as compared to the first (CO) absorption of **1**, are observed (Fig. S3(b)†). The shift of 77 $cm^{-1}$ for the band at 2097 $cm^{-1}$ is identical with the typical $\nu$(CO) band shift (*ca.* 70–100 $cm^{-1}$) for the formation of the μ-hydride diiron species from analogous diiron complexes,[6,7,9–12] and the shift of 13 $cm^{-1}$ for the band at 2033 $cm^{-1}$ is similar to that reported for the N-protonated diiron complexes.[1–4,6] The shifts of the $\nu$(CO) bands suggests that the singly protonated $[\mathbf{1}(H_\mu)]^+$ and $[\mathbf{1}(H_N)]^+$ might be concomitantly formed in the solution. Upon addition of HOTf up to 3 equiv., the $\nu$(CO) bands for **1**, $[\mathbf{1}(H_\mu)]^+$ and $[\mathbf{1}(H_N)]^+$ disappear completely and four new $\nu$(CO) bands appear with a shift of 85 $cm^{-1}$ for the first $\nu$(CO) band to higher frequency (Fig. S3(e)†), indicative of the transformation of $[\mathbf{1}(H_\mu)]^+$ and $[\mathbf{1}(H_N)]^+$ to $[\mathbf{1}(H_NH_\mu)]^{2+}$.

The protonation process of **1** was also monitored by *in situ* $^1H$ and $^{31}P\{^1H\}$ NMR spectroscopy. Complex **1** displays only one $^{31}P$ signal at $\delta$ = 52.5 (Fig. 2(a′)) in $d_6$-acetone, attributed to the apical–basal isomer of **1** in light of the X-ray analysis of its single crystal. As 1 equiv. of HOTf is added to the solution of **1**, two additional signals appear in the $^1H$ NMR spectrum (Fig. 2(b)). The high-field triplet at $\delta$ = −13.0 ($J_{H-P}$ = 20 Hz) unambiguously arises from the μ-hydride diiron complex $[\mathbf{1}(H_\mu)]^+$ and the low field broad signal at $\delta$ = 8.6 from the proton on the nitrogen atom ($H_N$) of $[\mathbf{1}(H_N)]^+$.[10,20] The corresponding $^{31}P$ NMR spectrum (Fig. 2(b′)) displays three additional signals at $\delta$ = 37.3, 57.7, and 58.4. The appearance or disappearance of $^{31}P$ signals at $\delta$ = 57.7 and 58.4 is always simultaneous with the $^1H$ signal at $\delta$ = 8.6 and the other $^{31}P$ signal at $\delta$ = 37.3 is accompanied, in every instance, by the $^1H$ signal at $\delta$ = −13.0. Therefore, the $^{31}P$ signals at $\delta$ = 57.7 and 58.4 are attributed to the $H_N$-*endo*/*exo* isomers of $[\mathbf{1}(H_N)]^+$ and the $^{31}P$ signal at $\delta$ = 37.3 is assigned to the phosphorus atoms of the μ-hydride complex $[\mathbf{1}(H_\mu)]^+$. Upon addition of one more equiv. of HOTf, the signal at $\delta$ = −13.0 for $[\mathbf{1}(H_\mu)]^+$ disappears, accompanied with the appearance of a broad signal at $\delta$ = −13.6 and a triplet at −13.9 ($J_{H-P}$ = 20 Hz, Fig. 2(c)). In addition to the two high-field signals, there are also two additional broad signals at $\delta$ = 8.6 and 10.1 in the low field of Fig. 2(c), attributed to the $H_N$ atoms of $[\mathbf{1}(H_N)]^+$ and $[\mathbf{1}(H_NH_\mu)]^{2+}$, respectively. Similarly, the signal at $\delta$ = 37.3 disappears in the $^{31}P$ NMR spectrum (Fig. 2(c′)), accompanied with the appearance of two additional signals at $\delta$ = 45.1 (broad) and 46.2, while the intensities of the signals at $\delta$ = 57.7 and 58.4 do not show apparent changes. The Fig. 2(c) and (c′) can be explained by coexistence of $[\mathbf{1}(H_NH_\mu)]^{2+}$ and $[\mathbf{1}(H_N)]^+$, both of which exist as $H_N$-*endo*/*exo* isomers.[20] Further addition of HOTf up to 3 equiv. results in immediate disappearance of the $^{31}P$ signals at $\delta$ = 57.7 and 58.4. Only the signals ascribed to the doubly protonated species are left in the $^1H$ and $^{31}P$ NMR spectra (Fig. 2(d) and (d′) at 298 K). At 218 K, two triplets in the high field for the $H_\mu$ and two corresponding signals at $\delta$ = 9.6 and 10.6 for the $H_N$ appear in the $^1H$ NMR spectrum (Fig. 2(e)). According to the intensities of the $^1H$ and $^{31}P$ signals, the $^1H$ signals at $\delta$ = −13.9 ($H_\mu$) and 10.6 ($H_N$) match with the $^{31}P$ signal at $\delta$ = 46.2, which are ascribed to the $H_N$-*endo* isomer of $[\mathbf{1}(H_NH_\mu)]^{2+}$, and the $^1H$ signals of low intensity at $\delta$ = −13.6 ($H_\mu$), 9.6 ($H_N$), and the $^{31}P$

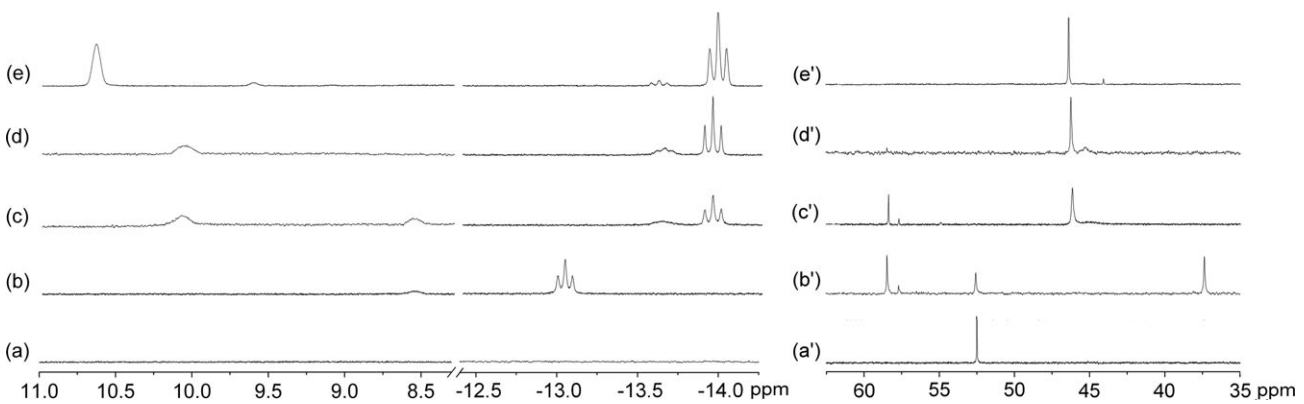


**Fig. 2** Selected regions of the $^1H$ and $^{31}P\{^1H\}$ NMR of **1** in $d_6$-acetone with (a, a′) + 0 equiv., (b, b′) + 1 equiv., (c, c′) + 2 equiv., (d, d′) + 3 equiv. HOTf at 298 K, and (e, e′) + 3 equiv. HOTf at 218 K.

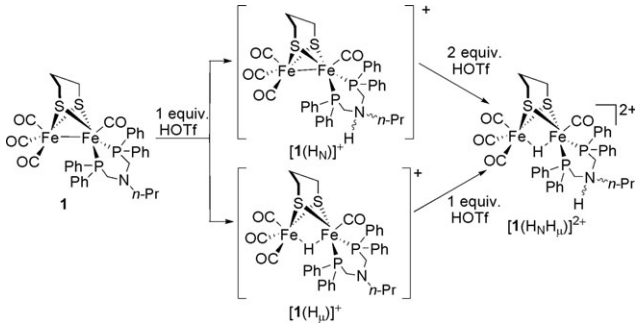

**Scheme 1** Protonation reactions of **1** with different amounts of HOTf.

signal at $\delta = 45.1$ are assigned to the $H_N$-*exo* isomer. The ratio of the $H_N$-*endo*/*exo* isomers of $[\mathbf{1}(H_NH_\mu)]^{2+}$ is 3.8 in $d_6$-acetone at 298 K (Fig. 2(d)). It is a rational argument that the $H_N$-*endo* isomer with the propyl group on the equatorial bond of the Fe(2)PCNCP cyclohexane ring is more stable than the $H_N$-*exo* isomer due to relief of the special congestion. In fact, the $H_N$-*endo* isomer is found in the solid state of $[\mathbf{1}(H_NH_\mu)]^{2+}$. The parent complex **1** is recovered when 6 equiv. of aniline is added.

In terms of the *in situ* IR, $^1$H and $^{31}$P NMR spectra, it can be concluded that in the presence of 1 equiv. of HOTf singly-protonated species $[\mathbf{1}(H_\mu)]^+$ and $[\mathbf{1}(H_N)]^+$ are formed competitively. Further protonation at the nitrogen atom of $[\mathbf{1}(H_\mu)]^+$ is preferred over that at the iron atoms of $[\mathbf{1}(H_N)]^+$ (Scheme 1). Double protonation of **1** in the presence of a slight excess of HOTf and complete deprotonation of $[\mathbf{1}(H_NH_\mu)]^{2+}$ in the presence of aniline are reversible, and the process occurs quantitatively.

Electrochemical studies show that complex **1** displays an irreversible reduction peak at $-2.33$ V *vs.* $Fc/Fc^+$ in dry $CH_2Cl_2$ (Fig. S4). Two additional reduction peaks, shifted by 1.08 and 0.6 V, respectively, emerge in the cyclic voltammogram upon addition of 1 equiv. of HOTf. According to previous reports,[2,6,9,11] the peak at $-1.28$ V is attributed to $[\mathbf{1}(H_\mu)]^+$ and the one at $-1.73$ V to $[\mathbf{1}(H_N)]^+$. With successive addition of HOTf up to 2.5 equiv., a new reduction peak appears at $-1.02$ V with a dramatic anodic shift of 1.31 V as compared to that for **1**, which is a reflection of the double protonation of **1**.

In summary, a proton–hydride diiron dithiolate complex containing an internal basic site in the diphosphine ligand has been successfully isolated and crystallographically characterized. The pendant base in the phosphine ligand of **1** may play a similar role to the proton-transfer relay as the bridging N in a diiron azadithiolate complex does. The $[\mathbf{1}(H_NH_\mu)]^{2+}$ displays a comparable anodic shift to the doubly-protonated diiron azadithiolate complex. The $H_\mu{}^-\cdots H_N{}^+$ distance (3.934 Å) in the proton–hydride model $[\mathbf{1}(H_NH_\mu)]^{2+}$ is considerably reduced compared to that in the doubly protonated μ-hydride species of diiron azadithiolate complexes. Intermediates with the proton and hydride close to each other are catalytically important for dihydrogen formation and uptake on transition metal-based homogeneous catalysts *via* an ionic mechanism. Further study on intra- and intermolecular hydride/proton exchange will be made for $[\mathbf{1}(H_NH_\mu)](OTf)_2$.

We are grateful to the Chinese National Natural Science Foundation (Grant no. 20633020), the Program for Changjiang Scholars and Innovative Research Team in University (IRT0711), the Swedish Energy Agency, the Swedish Research Council, and K & A Wallenberg Foundation for financial support of this work.

## Notes and references

‡ Crystal data for **1**: $C_{36}H_{37}Fe_2NO_4P_2S_2$, $M = 785.43$, triclinic, space group $P\bar{1}$, $a = 11.1157(9)$ Å, $b = 11.4433(8)$ Å, $c = 14.6215(11)$ Å, $\alpha = 98.316(5)^\circ$, $\beta = 100.308(5)^\circ$, $\gamma = 97.616(5)^\circ$, $U = 1786.5(2)$ Å$^3$, $T = 298$ K, $Z = 2$, $\mu = 1.058$ mm$^{-1}$, 15 635 reflections measured, 6221 unique (used in all calculations), $R_{int} = 0.0565$, final $R(F^2) = 0.0429$, and final w$R(F^2) = 0.0941$ (all data). CCDC 693384.
Crystal data for $[\mathbf{1}(H_NH_\mu)](OTf)_2{\cdot}H_2O$: $C_{38}H_{41}F_6Fe_2NO_{11}P_2S_4$, $M = 1103.60$, monoclinic, space group $C2/c$, $a = 37.62(2)$ Å, $b = 11.521(7)$ Å, $c = 21.396(14)$ Å, $\beta = 92.072(8)^\circ$, $U = 9267(10)$ Å$^3$, $T = 298$ K, $Z = 8$, $\mu = 0.956$ mm$^{-1}$, 21 888 reflections measured, 8159 unique (used in all calculations), $R_{int} = 0.0625$, final $R(F^2) = 0.0488$, and final w$R(F^2) = 0.1021$ (all data). CCDC 693385. For crystallographic data in CIF or other electronic format see DOI: 10.1039/b811352a

1 J. D. Lawrence, H. Li, T. B. Rauchfuss, M. Bénard and M.-M. Rohmer, *Angew. Chem., Int. Ed.*, 2001, **40**, 1768–1771.
2 S. Ott, M. Kritikos, B. Åkermark, L. Sun and R. Lomoth, *Angew. Chem., Int. Ed.*, 2004, **43**, 1006–1009.
3 P. Das, J.-F. Capon, F. Gloaguen, F. Y. Pétillon, P. Schollhammer and J. Talarmin, *Inorg. Chem.*, 2004, **43**, 8203–8205.
4 F. Wang, M. Wang, X. Liu, K. Jin, W. Dong, G. Li, B. Åkermark and L. Sun, *Chem. Commun.*, 2005, 3221–3223.
5 F. Xu, C. Tard, X. Wang, S. K. Ibrahim, D. Hughes, W. Zhong, X. Zeng, Q. Luo, X. Liu and C. J. Pickett, *Chem. Commun.*, 2008, 606–608.
6 L. Schwartz, G. Eilers, L. Eriksson, A. Gogoll, R. Lomoth and S. Ott, *Chem. Commun.*, 2006, 520–522.
7 G. Eilers, L. Schwartz, M. Stein, G. Zampella, L. de Gioia, S. Ott and R. Lomoth, *Chem.–Eur. J.*, 2007, **13**, 7075–7084.
8 H.-J. Fan and M. B. Hall, *J. Am. Chem. Soc.*, 2001, **123**, 3828–3829.
9 F. Gloaguen, J. D. Lawrence and T. B. Rauchfuss, *J. Am. Chem. Soc.*, 2001, **123**, 9476–9477.
10 X. Zhao, I. P. Georgakaki, M. L. Miller, R. Mejia-Rodriguez, C.-Y. Chiang and M. Y. Darensbourg, *Inorg. Chem.*, 2002, **41**, 3917–3928.
11 F. Gloaguen, J. D. Lawrence, T. B. Rauchfuss, M. Bénard and M.-M. Rohmer, *Inorg. Chem.*, 2002, **41**, 6573–6582.
12 D. Morvan, J.-F. Capon, F. Gloaguen, A. L. Goff, M. Marchivie, F. Michaud, P. Schollhammer, J. Talarmin and J.-J. Yaouanc, *Organometallics*, 2007, **26**, 2042–2052.
13 T. Zhou, Y. Mo, A. Liu, Z. Zhou and K. R. Tsai, *Inorg. Chem.*, 2004, **43**, 923–930.
14 G. Zampella, C. Greco, P. Fantucci and L. De Gioia, *Inorg. Chem.*, 2006, **45**, 4109–4118.
15 J. I. van der Vlugt, T. B. Rauchfuss, C. M. Whaley and S. R. Wilson, *J. Am. Chem. Soc.*, 2005, **127**, 16012–16013.
16 S. Ezzaher, J.-F. Capon, F. Gloaguen, F. Y. Pétillon, P. Schollhammer and J. Talarmin, *Inorg. Chem.*, 2007, **46**, 3426–3428.
17 B. E. Barton and T. B. Rauchfuss, *Inorg. Chem.*, 2008, **47**, 2261–2263.
18 C. J. Curtis, A. Miedaner, R. Ciancanelli, W. W. Ellis, B. C. Noll, M. R. DuBois and D. L. DuBois, *Inorg. Chem.*, 2003, **42**, 216–227.
19 G. M. Jacobsen, R. K. Shoemaker, M. R. DuBois and D. L. DuBois, *Organometallics*, 2007, **26**, 4964–4971.
20 R. M. Henry, R. K. Shoemaker, D. L. DuBois and M. R. DuBois, *J. Am. Chem. Soc.*, 2006, **128**, 3002–3010.

 